Proceedings of The Institute of Acoustics

SEA SURFACE WAVE-HEIGHT EFFECTS ON SHALLOW WATER MATCHED-FIELD PROCESSING

Donald R. Del Balzo (1), Christopher Feuillade (2) and Mary M. Rowe (2)

(1) Naval Ocean Research and Development Activity, NSTL, MS 39529-5004, USA
(2) ODSI Defense Systems, Inc., 6110 Executive Blvd., Rockville, MD 20852, USA

INTRODUCTION

The use of matched-field techniques for underwater acoustic detection and localization has been a subject of keen interest and debate over the last 2-3 years. Essentially, the technique involves the correlation of the acoustic pressure field signal detected at each receiver in a hydrophone array due to a submerged source, with the field calculated at the receiver based upon an estimated source position and an assumed model of the geoacoustic environment. A high degree of correlation between the experimental and model fields should indicate an increased probability of finding the source at the estimated position.

A number of different mathematical estimator functions may be employed to make the comparisons between the experimental and model fields. Perhaps the most straightforward of these is a conventional cross-correlation of the two sets of complex pressure values. A good discussion of this method has been given by Heitmeyer et al. [1]; and another similar technique has been described by Bucker [2].

Much more attention has been given to the maximum likelihood estimator, first introduced for use in a seismic array by Capon et. al. [3]. This method was adapted for depth estimation in a waveguide by Hinich [4]; and successful experimental trials employing it for localization in depth and range have been reported in shallow-water [5] and deep-water, arctic [6] environments. The maximum likelihood estimator shows great promise as a high-resolution localization tool. However, there are some important questions to be answered concerning its robustness and reliability when the environmental data used to calculate the model acoustic pressure field are incomplete or inaccurate, so that a data 'mismatch' occurs between the experimental and model pressure fields.

In this paper we investigate the consequences for the maximum-likelihood function, of one important type of mismatch, which arises due to the occurrence of fluctuations in the sea-surface height. Since almost all computer codes commonly used to generate the model field (whether range-dependent or range-independent) assume a flat sea-surface, this type of mismatch will invariably occur. In a shallow-water environment, for the waveguide depths and acoustic frequencies we are considering here, the hydrophone spacing in the array would normally be $\sim$1-2 meters. Since sea-surface waves with a peak-to-peak amplitude within this range are not unusual, mismatches in water depth equal to or greater than the hydrophone spacing will frequently be encountered. Clearly, any phenomenon which can significantly affect the phase relationships between the hydrophones, and therefore the accuracy of the beamforming process, must be investigated and understood.

THEORY

As mentioned above, the matched-field technique considered here is the maximum-likelihood estimator. For a full description of this method the reader is referred to a standard text [7]. Here we will provide only a brief summary of the basic theory.

Let the complex acoustic pressure field recorded at the n^{th} element of a vertical hydrophone array due to a source located at depth and range (z_o, r_o) be given by P_n'. We may write down a matrix row vector $\tilde{X}$ (the tilde denotes the transpose) of length N (the total number of hydrophones) whose individual members are the pressure fields recorded at those hydrophones

$$\tilde{X} = (P_1', P_2', \ldots, P_N') \tag{1}$$

From this we may form the cross-spectral (or covariance) matrix

$$R = XX^\dagger \tag{2}$$

Now consider another row vector $\tilde{E}$, whose members are the complex pressure fields P_n'' calculated at each hydrophone due to an estimated source position $(\hat{z}_o, \hat{r}_o)$, and normalized to unity. Therefore

$$\tilde{E} = (\overline{P}_1'', \overline{P}_2'', \ldots, \overline{P}_N'') \tag{3}$$

where,

$$\overline{P}_j'' = P_j'' \Big/ \left(\sum_{i=1}^{N} \left| P_i'' \right|^2 \right)^{1/2} \tag{4}$$

Usually a mean cross-spectral matrix is found by averaging over the total number M of recorded time-samples

$$\overline{R} = (1/M) \sum_{k=1}^{M} R_k \tag{5}$$

Noise on the hydrophones is simulated by adding a constant δ to each of the diagonal elements of R. This constant is scaled to give the desired signal to noise ratio. Now the maximum likelihood function may be written

$$L(z_o, \hat{z}_o; r_o, \hat{r}_o) = 1/(E^\dagger(\overline{R})^{-1}E) \tag{6}$$

We can see from the matrix expression in the denominator of (6) that determining the value of the maximum likelihood function involves calculating products of functions of the model pressure field $\overline{P}_j''$ (in E) and functions of the measured pressure field P_n' (in R). If the model field and measured field correspond closely with each other for every individual hydrophone, then the denominator in (6) will be small, and hence L will take a large value. However, if a mismatch in the sea-surface wave-height comparable to the hydrophone spacing occurs, then a significant phase error will be introduced into the calculated model value of the pressure field at each hydrophone. These may then differ seriously from the measured field values for the corresponding hydrophones, leading to a detrimental effect on the value of L calculated in (6).

ENVIRONMENTAL MODEL

The geoacoustic environmental model used in this work is the two-layered liquid half-space model pioneered by Pekeris [8]. The model consists of a shallow isospeed water layer of uniform density overlying a faster, isospeed, semi-infinite fluid bottom of uniform (and usually higher) density. For a full description of the model the reader is refered to a standard text [9]. Even though the simplicity of the Pekeris model limits its general applicability, it does possess features which are closely similar to at least one shallow water environment in which matched-field experiments have been performed [5]: where the water sound speed profile is almost isospeed and where a thick sandy sediment layer is present which carries no shear waves and therefore behaves like a fluid. The Pekeris model is also a widely used and well-understood standard model. It should exhibit most of the phenomena which occur in shallow-water environments due to the presence of surface wave-height fluctuations. Since the acoustic wavefunctions within the waveguide are calculated analytically, without need for recourse to numerical techniques, the calculation of the maximum likelihood function in (6) is greatly facilitated, making the Pekeris model an excellent choice for our present purposes.

SEA-SURFACE FLUCTUATION MODELING

It is clear that the variations in surface wave-height under typical sea conditions will be generally random and difficult to model analytically. There are no propagation codes which allow for the introduction of randomly varying wave-height available at the present time. In order, therefore, to approach the problem of the effect of variable sea-surface height on the maximum-likelihood estimator using the Pekeris model, we have made two simplifying assumptions. The first of these is to study the effects of waveheight mismatch due to ocean swell. The relationship between wind waves and swell has been the subject of extensive investigation, and a comprehensive review of it has been given by Wiegel [10]. Since the ocean is a dispersive medium as far as surface-waves are concerned, waves of different periods generated by a storm travel away from it at different speeds. The waves with the longest period travel most quickly. At a distance of a few storm diameters from their origin, the waves will propagate independently of each other, and are characterised by a sinusoidal wave form on the ocean surface. In this work we have considered the effects of an ocean swell of peak-to-trough amplitude 7 meters. Since this is about the greatest swell amplitude recorded [11], we may consider it a 'worst case' estimate. The second simplification we have made is to utilise a 'long-crested' model of the ocean-surface, and to assume that sound propagates from the source to the array of receivers along paths parallel to the crests. Since we are considering ranges $\sim$5-7 km, we are dealing with acoustic transit times from source to receivers of $\sim$3-4 s. Earle et al [11] have recorded that swells of the order we are considering have periods of about 20-25 s. Hence it seems reasonable for us to use a 'frozen ocean' assumption; and to neglect the small change in surface height which occurs as the signal propagates from the source to the hydrophone array along the ocean crests. This allows us to model the effect of the sinusoidal wave-height variation by taking the mean of a series of static cases each representing a different phase of the surface wave.

FLUCTUATION MODELING PROCEDURE

In this work we consider the localization of a 150 Hz source placed in a waveguide of water depth 100m, at a range of 4000m. The sound speed in the water and sediment are 1500 m/s and 1621.6 m/s respectively. The sediment/water density ratio is 1.772. The effect of swell on matched-field processing of shallow water data is, for modeling purposes, equivalent to the effect of under- or over-estimating the water depth by an amount equal to the height or depth of the wave profile. The sinusoidal profile of the swell is therefore approximated by sampling 72 points equally angularly spaced at intervals of 5° along a sine wave of amplitude 3.5m. The overall effect of the swell on the localization function is then modeled by taking the mean of a set of discrete cases of successively increasing waveheights, representing waveheight mismatches between -3.5m and +3.5m.

The pressure fields at the hydrophone array due to source positions within a range interval of 1000m to 7000m and a depth interval of 0m to 100m were obtained using the Pekeris waveguide model. Instead of calculating the field at the receiver array due to a source at each point in the search grid, the field was calculated at all the grid points due to a source at each receiver location, and acoustic propagation reciprocity was assumed. By this means the number of modeling runs was greatly reduced. Horizontal and vertical grid point separations were chosen based on the size of the targets to be localized. Finer grid spacings would then serve only to increase computation time without significantly increasing localization accuracy. The receiver array used for modeling spanned the central 50m of the 100m water column. In order to adequately sample the 150 Hz signal, 21 hydrophones, 2.5m apart, were chosen to make up the array.

A synthetic set of "measured" data for each of the 37 discrete swell heights was generated by running the Pekeris model to obtain the field at the receiver array due to a source at the desired location. The water depth used in this instance was equal to the 100m modeled depth plus (or minus) the swell height. For each waveheight case the ambiguity surface was produced by applying the maximum likelihood estimator to the model field and to the synthetic data. A composite of these surfaces, representing the results obtained by applying matched-field processing to time averaged data, was compiled by adding the ambiguity surfaces for the individual cases and then taking the mean. All the surfaces were plotted on a decibel scale.

Peak values (P) and mean background levels (μ) were calculated for each surface. The mean level was calculated by excluding an 11 point by 11 point box surrounding the peak value on the surface and an 11 point by 11 point box surrounding the actual source point. Also calculated were values of $(P-\mu)/\mu$, both for the overall peak of the ambiguity surface, and the peak found within the 11 point by 11 point box surrounding the source point. The constant δ, scaled to give a signal to noise ratio of 10 dB, was added to each of the diagonal elements of R. A high ratio was used so as to effectively eliminate signal to noise considerations from the problem, and to allow the effects of sea-surface mismatch to predominate.

RESULTS

We have investigated the effects of mismatch upon localization of sources placed at three distinct depths within the 100m waveguide: at 24.7m; at 49.2m; and at 74.9m. In figures 1(a) - 1(c) are shown, in isometric projection, the ambiguity surfaces generated by the maximum-likelihood estimator for sources at these locations, assuming a flat ocean surface. No mismatch between the model and "measured" sea-surfaces has yet been introduced. In each case the source peaks may be clearly and unmistakably seen set against a background of lower secondary peaks. The value of $(P-\mu)/\mu$ for these surfaces is about 21 dB for all three. This is plotted in figure 2(a), which also shows the variation in $(P-\mu)/\mu$ as sea-surface mismatch (still assuming a flat surface) increases in both the positive and negative direction. Inspection of figure 2(a) shows that for all three source depth cases the value of $(P-\mu)/\mu$ oscillates strongly, but shows a general tendency to decrease as the degree of mismatch increases. However, for the relatively small mismatch of $\pm$1m ($\sim\pm$1% of the total depth) the value of $(P-\mu)/\mu$ has fallen between 9 to 11.5 dB on the positive side and between 14 to 19 dB on the negative side. As the mismatch increases still further, in both directions, the value of $(P-\mu)/\mu$ tends to vary between about 2.5 and 17.5 dB. This indicates that, depending upon degree of mismatch, the source peak may still be identifiable, but will have an increasing tendency to be obscured by the noise background as mismatch increases. In figure 2(b) is shown the variation in range error as a function of mismatch. Inspection of this figure indicates that as the sea-surface mismatch increases from negative to positive values, the range error tends to decrease linearly and monotonically for all source depths. This means that if the water depth is overestimated in the model data, there will always be a tendency to localize the source further away than it actually is. If the water depth is underestimated, the source will appear too close. The figure shows that for a waveheight mismatch of $\pm$3.0m ($\sim\pm$3% of the total water depth) the range error for this environment will be $\mp$250.0m ($\sim\mp$6.2% of the actual range). It will be noted that a few anomalous points do not fall on the main linear sequence on the negative waveheight side of figure 2(b). This is due to the loss of one of the trapped normal modes at a mismatch of $\leqq$ -0.8m. The value of $(P-\mu)/\mu$ falls to between 7 to 11 dB (see figure 2(a)), and the source peak cannot, in some cases, be accurately identified from among many background peaks of similar height (sometimes called "false" targets). In figure 2(c) is shown the variation in depth error as a function of mismatch. Apart from some obviously anomalous points at negative mismatch values (which arise for the same reason as in figure 2(b)) there is a small tendency for the depth error to increase from a negative to a positive value as the sea-surface mismatch increases in the same direction. Therefore, if the water-depth is overestimated, there will be a tendency to localize the source shallower than it actually is, and vice versa. Inspection of the figure shows, however, that any depth errors introduced by sea-surface mismatch are proportionally much smaller than the corresponding range errors.

In figures 3(a) - 3(c) are shown the composite ambiguity surfaces, calculated by taking the mean of the 72 surfaces for the individual waveheights at 5° intervals on the sine wave, as described earlier, for source depths of 24.7m, 49.2m and 74.9m respectively. Inspection of these surfaces reveals that the source peaks, although degraded in quality against the corresponding peaks

1(a)

1(b)

1(c)

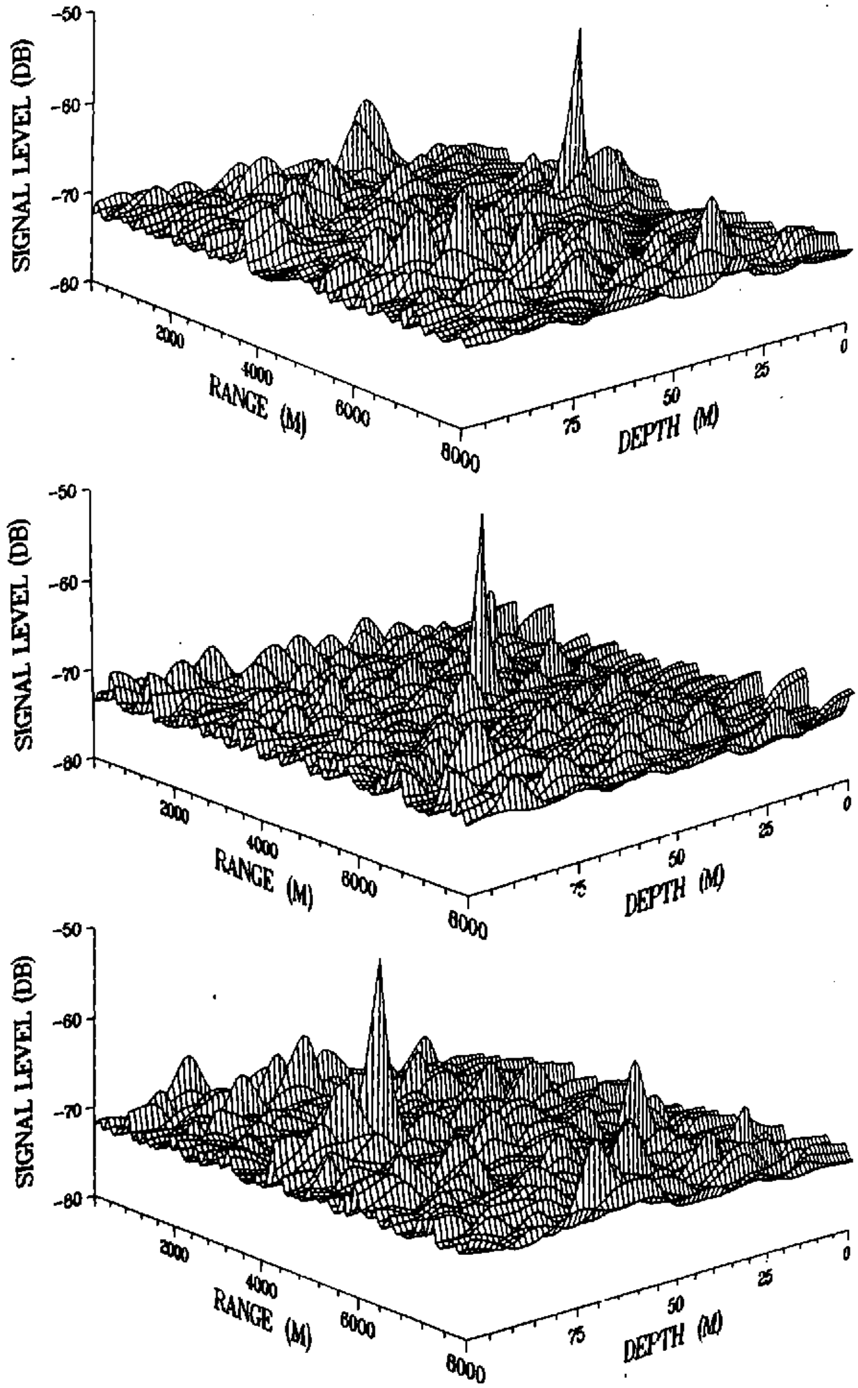

Figures 1(a), 1(b), 1(c). Ambiguity surfaces are shown for a 150 Hz source placed at depths of: (a) 24.7m, (b) 49.2m, and (c) 74.9m, in a 100m Pekeris waveguide. The sea-surface is assumed flat, and there is no mismatch. The input signal to noise ratio is 10 dB. The maximum-likelihood signal level is expressed in dB.

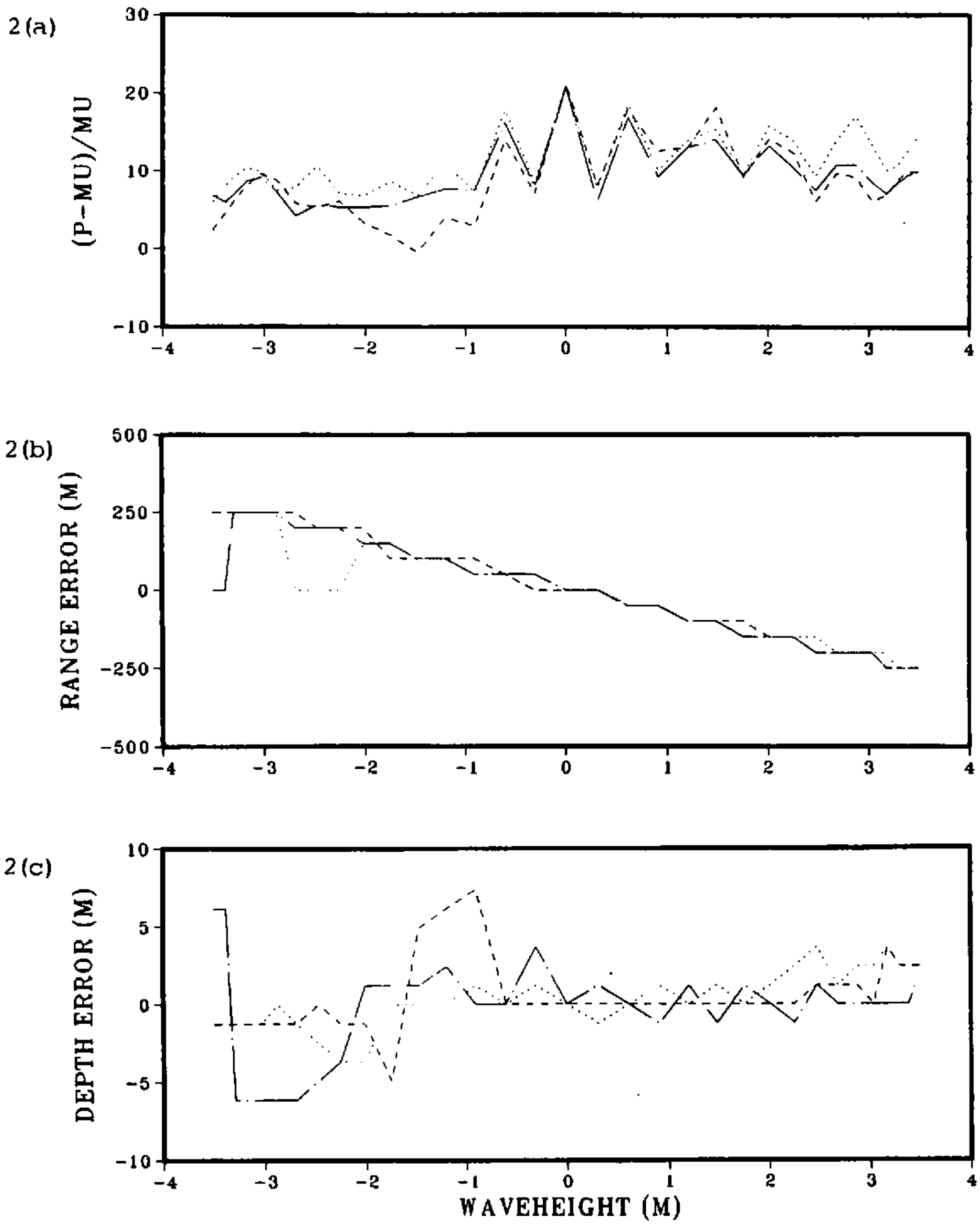

Figure 2(a), 2(b), 2(c). These graphs show the variation in: (a) $(P-\mu)/\mu$ (in dB), (b) range error, and (c) depth error, as a function of sea-surface mismatch expressed as waveheight (in meters). The 24.9m source depth case is represented by a dotted line in all three graphs, the 49.2m case is represented by a dashed line, the 74.9m case by a dot-dashed line.

3(a)

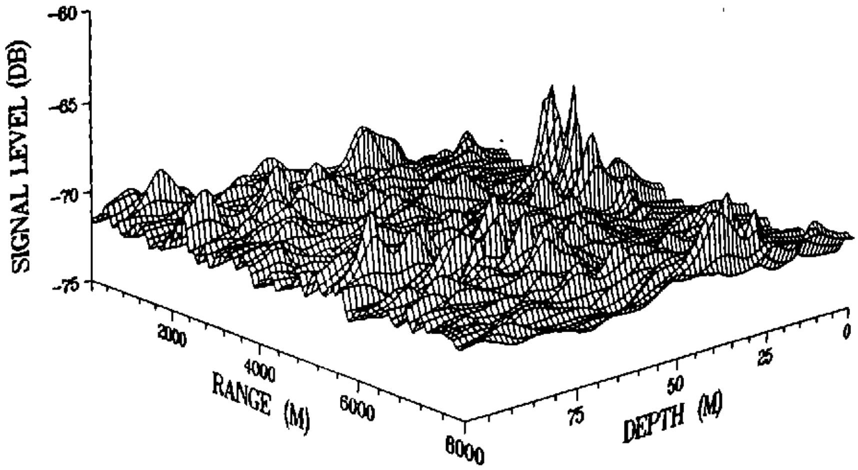

3(b)

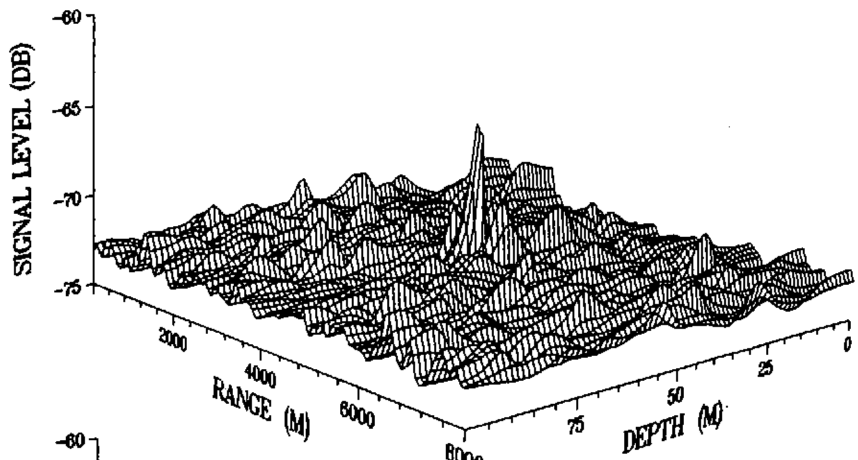

3(c)

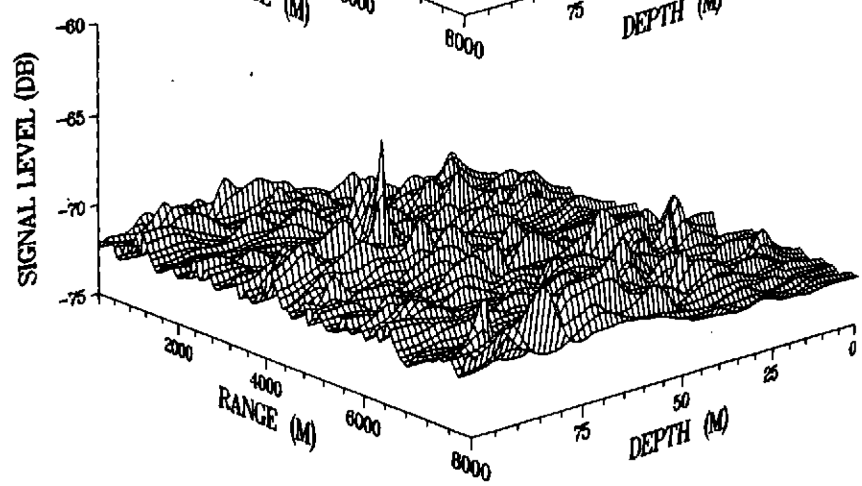

Figures 3(a), 3(b), 3(c). Composite ambiguity surfaces for source depth cases: (a) 24.7m, (b) 49.2m, and (c) 74.9m. The frequency is 150 Hz, and the signal to noise ratio is 10 dB. The maximum-likelihood 'signal' level is expressed in dB.

for the zero waveheight case in figures 1(a) - 1(c), are still quite identifiable. Whereas the peaks in figures 1(a) - 1(c) all had a value of $(P-\mu)/\mu$ of around 21 dB, the values here are: 6.19 dB for the 24.7m case; 6.88 dB for the 49.2m case; and 10.55 dB for the 74.9m case. When comparing figures 3(a) - 3(c) with figures 1(a) - 1(c), the change of scale on the signal level axis should be noted. This shows a decrease in $(P-\mu)/\mu$ of $\sim$10 to 15 dB for the composite peaks.

The explanation for the fact that the composite peaks are not more degraded than we might expect is implicit in figure 2(a). For relatively small surface mismatches ($\sim$ 1-3m), we have seen that the amplitude of the peak falls by 10 dB or more. This means that when the mean of the 72 surfaces is taken to obtain the composite, the surfaces for the more extreme mismatches (1-3m) will contribute relatively little in comparison to those for near-zero ($<$ 1m) mismatches. Since the more extreme cases give rise to the greatest problems in peak identification and range and depth errors, the fact that they are quite naturally de-emphasized is fortunate. Processing of the composite surfaces reveals zero range and depth errors for all three source depth cases, with the single exception of a range error of -100m in the 49.2m case.

CONCLUSIONS

We have seen that, in a shallow water environment, significant errors can be introduced into the range and depth localization predictions of a matched-field processor through erroneous estimates of the water depth. If the water depth is over-estimated, the processor will localize the source too far away and too shallow. If the depth is underestimated, the source will be seen too close and too deep. In the case examined here, range errors appear to be significantly greater than depth errors.

For a composite ambiguity surface, representing an average over many cycles of a sinusoidal ocean swell, the loss in performance of the matched-field processor is not as bad as seems to be suggested by the more extreme static mismatch cases. This is because output signal to noise ratio is dominated by the zero and near-zero mismatch ambiguity surfaces, for which range and depth errors are small. It is not an unreasonable extension to suppose that this argument will also hold true even for more extreme sea-state conditions, suggesting that matched-field processors may be useful over a large range of surface conditions.

ACKNOWLEDGEMENTS

This work was supported by the Bottom Interaction Program at NORDA. Graphical Software Support was furnished by Henry Rosche III. The authors wish to acknowledge the oceanographic advice of R. L. Pickett. They also wish to thank Lonnia Martin and Rachel Schmitt for invaluable typing assistance.

REFERENCES

[1] R.M. Heitmeyer, W. B. Moseley and R. G. Fizell, 'Full field ambiguity processing in a complex shallow water environment,' pp. 171-188 in High-Resolution Spatial Processing in Underwater Acoustics, R. A. Wagstaff and A. B. Baggeroer (editors), U.S. Govt. Pub. 1985.

[2] H. P. Bucker, 'Use of calculated sound fields and matched-field detection to locate sound sources in shallow water,' J.A.S.A., Vol. 59, no. 2, 368-373, (1976).
[3] J. Capon, R. J. Greenfield and R. J. Kolker,' Multidimensional maximum-likelihood processing of a large aperture seismic array,' Proc. IEEE, Vol. 55, 192-211, (1967).
[4] M. J. Hinich, 'Maximum-likelihood signal processing for a vertical array,' J.A.S.A., Vol. 54, no. 2, 499-503, (1973).
[5] C. Feuillade and W. A. Kinney, 'Source localization using a matched-field technique,' J.A.S.A., Vol. 78, Suppl. 1, 530, (1985).
[6] R. G. Fizell and S. C. Wales, 'Source localization in range and depth in an Arctic environment,' J.A.S.A., Vol. 78, Suppl. 1, 557, (1985).
[7] E. R. Kanasewich, 'The maximum likelihood method of spectral estimation,' pp. 177-183 in Time Sequence Analysis in Geophysics, Univ. of Alberta Pub. 1981.
[8] C. L. Pekeris, 'Theory of propagation of explosive sound in shallow water,' Geol. Soc. Am. Mem., no. 27, pp. 43-64, (1948).
[9] L. E. Kinsler, A. R. Frey, A. B. Coppens and J. V. Sanders, Fundamentals of Acoustics, 3rd edition, ch. 15, pp. 434-440, J. Wiley and Sons Pub. 1982.
[10] R. L. Wiegel, Oceanographical Engineering, ch. 9, pp. 195-237, Prentice-Hall Pub. 1964.
[11] M. D. Earle, K. A. Bush and G. D. Hamilton, 'High-height long-period ocean waves generated by a severe storm in the Northeast Pacific Ocean during February 1983,' J. Phys. Ocean., Vol. 14, 1286-1299, (1984).